



Extracting the hexadecapole deformation from backward quasi-elastic scattering

H. M. Jia, C. J. Lin,* F. Yang, X. X. Xu, H. Q. Zhang, Z. H. Liu, Z. D. Wu, L. Yang, N. R. Ma, P. F. Bao, and L. J. Sun

China Institute of Atomic Energy, P. O. Box 275(10), Beijing 102413, P. R. China

(Received 5 June 2014; revised manuscript received 25 August 2014; published 3 September 2014)

Background: The hexadecapole deformation β_4 is usually difficult to determine experimentally, especially its sign. The rapidly accumulated knowledge of β_2 inspires the desire of β_4 for radioactive nuclei, but the current low-quality beam is a severe experimental challenge. Therefore, a simple but sensitive method to extract β_4 in such a condition is urgently called for.

Purpose: To study the feasibility of extracting β_4 from the lower-energy backward quasi-elastic (QEL) scattering.

Methods: The QEL scattering at sub-barrier energy region is sensitive to the coupled-channels (CC) effect and consequently may be used to extract β_4 . The QEL scattering excitation functions for $^{16}\text{O} + ^{152}\text{Sm}$, ^{170}Er , and ^{174}Yb were measured at a backward angle with small energy intervals at energies near the Coulomb barrier. Experimental fusion barrier distributions were also derived. The lower-energy data were analyzed to extract β_4 with the help of the CC calculations.

Results: The obtained β_4 agrees with the available results reasonably well.

Conclusions: We have demonstrated that the QEL scattering at sub-barrier energies provides a feasible and sensitive method to extract the value of β_4 , which is essentially meaningful for the radioactive nucleus because of its low beam intensity.

DOI: [10.1103/PhysRevC.90.031601](https://doi.org/10.1103/PhysRevC.90.031601)

PACS number(s): 25.70.Bc, 24.10.Eq

The role played by nuclear structure in near-barrier heavy-ion fusion reactions has been observed several decades ago [1] and has been described well within the coupled-channels (CC) framework [2]. The coupling of the relative motion to nuclear intrinsic degrees of freedom gives rise to a distribution of fusion barriers instead of a single barrier [3]. Experimentally, barrier distribution can be extracted from the precise fusion excitation function by using the second derivative of $E\sigma_{\text{Fus}}$ [4], such as for $^{16}\text{O} + ^{154}\text{Sm}$ [5], $^{58}\text{Ni} + ^{60}\text{Ni}$ [6], and $^{16,17}\text{O} + ^{144}\text{Sm}$ [7]. Later, it was shown that a representation of barrier distribution can be extracted also from quasi-elastic (QEL) scattering measured at backward angles [8]. Here, QEL is defined as the sum of the elastic scattering and all other peripheral reaction processes [9].

Beside the quadrupole deformation β_2 effect, the possible role of static higher order hexadecapole deformation β_4 in the sub-barrier fusion has been frequently addressed [3,10–13]. The shapes are equivalent to those obtained classically from random orientation of the deformed nuclei [14], and β_4 is expected to have a significant effect on fusion. The differences in experimental fusion barrier distributions of $^{16}\text{O} + ^{186}\text{W}$ and $^{16}\text{O} + ^{154}\text{Sm}$ [15] mean that fusion reactions are very sensitive to not only β_2 but also small β_4 , where β_4 was varied to fit the lower-energy fusion data for $^{16}\text{O} + ^{186}\text{W}$. A good agreement of β_4 with the values extracted from Coulomb excitation was obtained for $^{16}\text{O} + ^{154}\text{Sm}$ [16] by using the same β_2 obtained from Coulomb excitation. Further, the sensitivity of the extracted deformation parameters to the couplings to the relatively weak vibrations and transfer channel in fitting the fusion excitation functions was pointed out [17].

Up to now, the methods of α scattering [18–21], electron scattering [22], and muonic x rays [23] were used to determine

the shape of deformed nucleus experimentally. The β_4 is difficult to extract experimentally, and all the results are model-dependent and quite different with big errors. Theoretically, the macroscopic-microscopic method [24,25] to calculate the ground-state deformation in both the Nilsson perturbed-spheroid and the spherical-harmonic expansions has been proposed [26].

According to the point of view that the backward QEL scattering is a process complementary to fusion, we attempt to extract β_4 by using the lower-energy QEL data where the deformation effect is expected to be dominant. Compared with fusion, QEL is easier to measure experimentally (and with high statistics), especially at the lower energy region.

A systematic variation of β_4 from positive in the light rare earths to negative in the heavy ones is established [21] through excitation of the ground rotational band by 50 MeV α particles. The general picture of the lanthanide nuclei is that β_4 drops from large positive values around +0.1 to large negative ones around -0.1 as the mass number A increases from 152 to 180. The crossover point of $\beta_4 = 0$ occurs around $A = 166$. The β_4 effect in sub-barrier fusion cross sections of $^{16}\text{O} + ^{154}\text{Sm}$, ^{166}Er , and ^{176}Yb [27] has been researched. A systematic research of β_4 evolution by using an independent method is needed to confirm this. Furthermore, with the increasing experimental β_2 knowledge and the availability of some low intensity radioactive beams [28–30], a sensitive method to extract β_4 of radioactive nuclei is urgently needed.

For this purpose, the spherical ^{16}O was selected as projectile. Good rotors, where the noncollective excitations are expected to be minor compared with the strong collective rotational states of ^{152}Sm , ^{170}Er , and ^{174}Yb were selected as target nuclei. They all have similar β_2 and excitation energies, but different β_4 for the ground-state rotational band.

The experiment was performed by using ^{16}O beam from the HI-13 tandem accelerator at China Institute of Atomic

*Corresponding author: cjlin@ciae.ac.cn

Energy (CIAE). The experimental method is similar to that of Ref. [31]. Thin targets ($50\text{--}100\ \mu\text{g}/\text{cm}^2$ thick) of ^{152}Sm , ^{170}Er , and ^{174}Yb with a diameter of 3 mm evaporated onto $20\text{--}25\ \mu\text{g}/\text{cm}^2$ carbon foils were used. The energy range is $E_{\text{Lab}} = 40\text{--}80$ MeV. The QEL particles were measured with four silicon surface barrier detectors placed symmetrically at the backward angle $\theta_{\text{Lab}} = 175^\circ$. Another group of four silicon surface barrier detectors were placed symmetrically at the forward angle $\theta_{\text{Lab}} = 41^\circ$ with respect to the beam axis to monitor the beam position and to normalize the cross section. In order to make a quantitative study of the barrier distribution, it is necessary to obtain QEL data with high accuracy. Several measures were taken to minimize the possible systematic uncertainties in the measurement.

The energy window for QEL was defined to include the elastic peak and the tail corresponding to all other peripheral processes. The cross sections of QEL were normalized with the counts of the Rutherford scattering in the four forward-angle monitor detectors. Energy loss in the carbon backing and target was considered in the data analysis.

The effective energy E_{eff} was used by considering the minor centrifugal energy E_{cent} correction, that is $E_{\text{eff}} = E_{\text{c.m.}} - E_{\text{cent}}$ with

$$E_{\text{cent}} = E_{\text{c.m.}} \frac{\text{cosec}(\theta_{\text{c.m.}}/2) - 1}{\text{cosec}(\theta_{\text{c.m.}}/2) + 1}, \quad (1)$$

in order to compare the barrier distribution $D_{\text{QEL}}(E_{\text{c.m.}}, 175^\circ)$ with $D_{\text{QEL}}(E_{\text{eff}}, 180^\circ)$. The corresponding experimental QEL scattering excitation functions obtained for the systems are plotted in the top panels of Figs. 1, 2, and 3 as solid points. The typical statistical errors are smaller than 1%.

The representation of the barrier distribution $D_{\text{QEL}}(E_{\text{eff}})$ was obtained by using the expression $D_{\text{QEL}} = -d(\sigma_{\text{QEL}}/\sigma_{\text{Ru}})/dE_{\text{eff}}$. An energy interval ΔE_{eff} about 2 MeV was used for the determination of the derivatives. The experimental barrier distributions obtained for the systems are plotted in the bottom panels of Figs. 1, 2, and 3 as solid points.

Considering the larger overlap of the reactants, and therefore strong absorption as well as distortion by nuclear force with increasing energy, only the lower energy data of $d\sigma_{\text{QEL}}/d\sigma_{\text{Ru}} > 0.7$ (corresponding to the low-energy side of the barrier distribution) was selected in the following analysis somewhat arbitrarily. The CC calculations were performed with a modified version of the code CCFULL [32]. A Woods-Saxon potential with the geometrical parameters of $r_{0V} = 1.20$ fm and $a_V = 0.65$ fm was used. The depth V was varied to reproduce the barrier energy determined from the QEL scattering excitation function at $d\sigma_{\text{QEL}}/d\sigma_{\text{Ru}} = 0.5$ [33], which is very close to the value extracted from fusion data. As usual, a short-range imaginary potential with $W = 30$ MeV, $r_{0W} = 1.0$ fm, and $a_W = 0.4$ fm was used to simulate the compound nucleus formation [34]. The calculated results are insensitive to the parameters of the imaginary part of the potential as long as it is strong enough and well localized inside the Coulomb barrier [35]. The used Coulomb radius parameter is $r_{0C} = 1.1$ fm, which has little influence on the cross section.

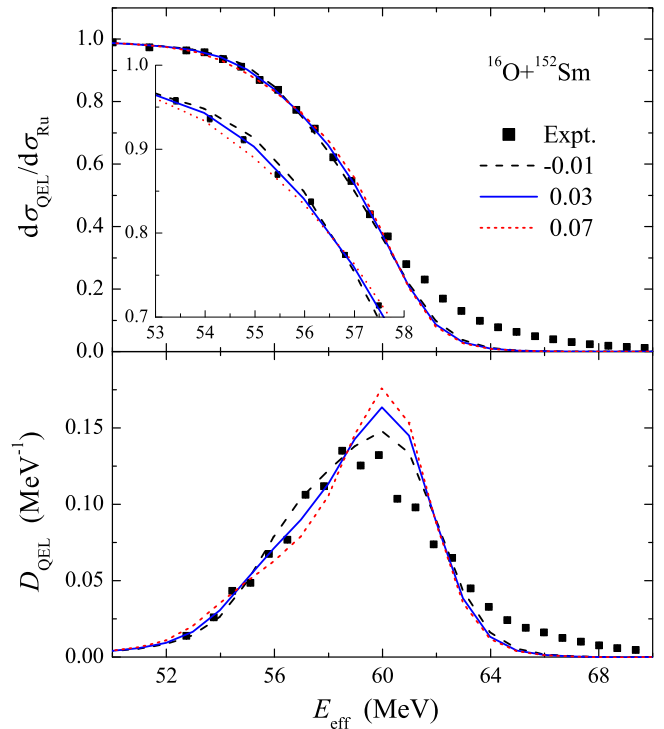


FIG. 1. (Color online) Experimental QEL scattering excitation function (top) and extracted barrier distribution D_{QEL} (bottom) for $^{16}\text{O} + ^{152}\text{Sm}$, compared with the CC calculation results by using different β_4 .

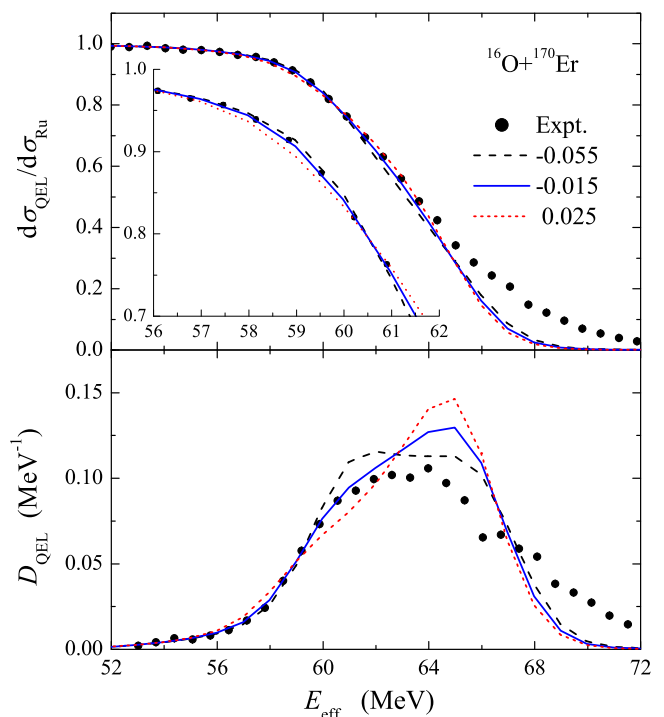


FIG. 2. (Color online) Same as in Fig. 1, but for $^{16}\text{O} + ^{170}\text{Er}$.

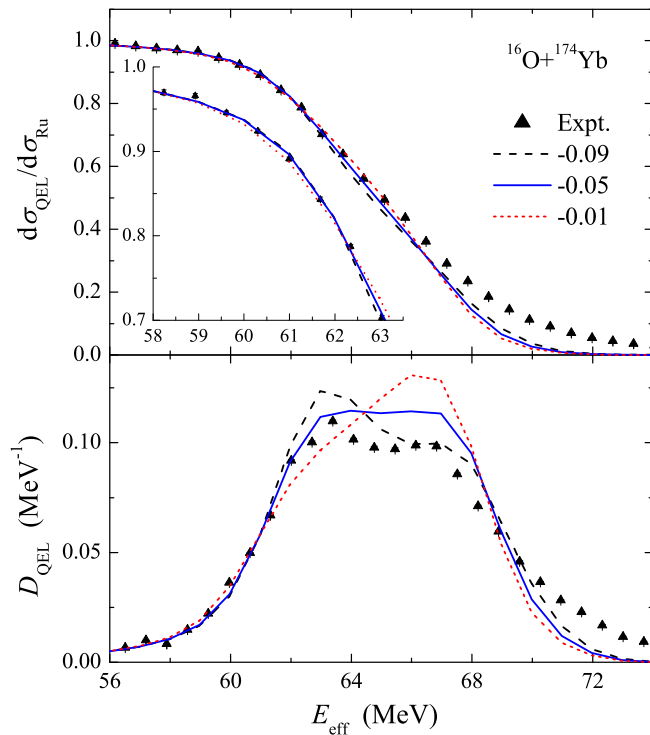


FIG. 3. (Color online) Same as in Fig. 1, but for $^{16}\text{O} + ^{174}\text{Yb}$.

The corresponding one-dimensional barrier potential parameters, i.e., the fusion-barrier energies, positions, and curvatures for the systems, are given in Table I. The excitation energies of ^{16}O are very high compared with the barrier curvature, so it only produces an adiabatic potential renormalization without affecting the structure of the barrier distribution [37]. This effect can be included in the potential and will not be considered explicitly in the CC calculations. Excitation states up to 10^+ in the rotational band of the target nuclei were included. Table I also lists the values [36] of the low-lying collective excitation states of the target nuclei. It should be mentioned that it is difficult to consider exactly the coupling to transfer channels in the CC calculations. Therefore, the coupling to transfer channels were not considered, assuming their minor effects at lower-energy region for the studied systems. In the following analysis, only β_4 was varied to fit the experimental data, while other parameters were fixed. The corresponding CC calculations with different β_4 are shown in Figs. 1, 2, and 3. The insertions in the figures

TABLE I. Excitation energies E^* and quadrupole deformation parameters β_2 [36] for the rotational states of the target nuclei included in the CC calculations, and the uncoupled barrier parameters for $^{16}\text{O} + ^{152}\text{Sm}$, ^{170}Er , and ^{174}Yb .

Target	E^* (keV)	β_2	V_B (MeV)	R_B (fm)	$\hbar\omega$ (MeV)
^{152}Sm	121.8	0.306	59.37	11.30	4.38
^{170}Er	78.6	0.336	63.69	11.58	4.48
^{174}Yb	76.5	0.325	65.41	11.60	4.52

show the enlargement of the effective fitting parts in the $d\sigma_{\text{QEL}}/d\sigma_{\text{Ru}} > 0.7$ region.

For $^{16}\text{O} + ^{152}\text{Sm}$, the CC calculation results with the same β_2 , but $\beta_4 = -0.01$ (dashed line), 0.03 (solid line), and 0.07 (dotted line) are plotted in Fig. 1 to illustrate its effect on the QEL scattering excitation function and barrier distribution. It can be seen that the CC calculation with $\beta_4 = 0.03$ fits the lower-energy QEL excitation function well. This also gives a good reproduction for the barrier distribution at lower energies, as shown in the bottom panel. This means that the lower energy QEL scattering is indeed sensitive to the higher order deformation and can be used to extract β_4 . The extracted β_4 for ^{152}Sm here agrees well with both $\beta_4^N = 0.038 \pm 0.007$ (with $\beta_2^N = 0.214 \pm 0.007$) extracted from 14–18 MeV α scattering [38] and 0.048 obtained from 50 MeV α scattering [21], but smaller than both the charge deformation parameter of $\beta_4^C = 0.08$ [39] and $\beta_4 = 0.07$ (with $\beta_2 = 0.287$) obtained from high-energy electron scattering data by using a deformed Fermi shape with a constant skin thickness for the nuclear shape [22].

For $^{16}\text{O} + ^{170}\text{Er}$, the data can be well reproduced with $\beta_4 = -0.015$ for both the lower energy QEL scattering and barrier distribution, as shown in Fig. 2. The CC calculation results with $\beta_4 = -0.055$ (dashed line) and 0.025 (dotted line) are also plotted. The extracted β_4 for ^{170}Er here agrees well with the value of $\beta_4 = -0.003$ extracted by using sub-barrier α scattering [40]. Also it is similar with the systematic calculation result of $\beta_4 = -0.023$ (with $\beta_2 = 0.296$) for the ground-state deformation of ^{170}Er based on the spherical-harmonics expansion [26].

Up to now, only fusion barrier distribution for the minus β_4 system of $^{16}\text{O} + ^{186}\text{W}$ has been obtained by using the precise fusion excitation function [15]. Indeed, the fusion barrier distribution shows a rapid rise in the sub-barrier energy region, which is expected from geometric considerations. ^{174}Yb is also expected to have a larger minus β_4 [26]. The barrier distribution for $^{16}\text{O} + ^{174}\text{Yb}$ in Fig. 3 really shows a shape similar to that of $^{16}\text{O} + ^{186}\text{W}$ [15].

The β_4 parameter, which gives a good reproduction for the lower energy QEL data of $^{16}\text{O} + ^{174}\text{Yb}$, is -0.05 for ^{174}Yb shown as the solid line in Fig. 3. Also the CC calculation results with $\beta_4 = -0.01$ (dashed line) and -0.09 (dotted line) are plotted. The results of QEL scattering excitation functions calculated using β_4 of -0.05 and -0.09 do not show a big difference, but the corresponding barrier distributions deviate evidently. The extracted β_4 for ^{174}Yb here agrees well with the average value of $\beta_4 = -0.037$ by using different methods [41], and $\beta_4 = -0.059$ (with $\beta_2 = 0.287$) based on the spherical-harmonics expansion [26]. It also agrees with the theoretical result of -0.05 (Woods-Saxon potential) [42]. But the value deviates from the charge deformation parameter $\beta_4^C = -0.007$ by using the precise Coulomb excitation with the shapes of both homogeneous and Fermi distributions [42].

Figures 1–3 demonstrate the influences of the β_4 values on the backward QEL excitation functions and the corresponding barrier distributions for the $^{16}\text{O} + ^{152}\text{Sm}$, ^{170}Er , and ^{174}Yb systems. The results represented by the solid curves are better than the others but may be not the best. In order to extract the

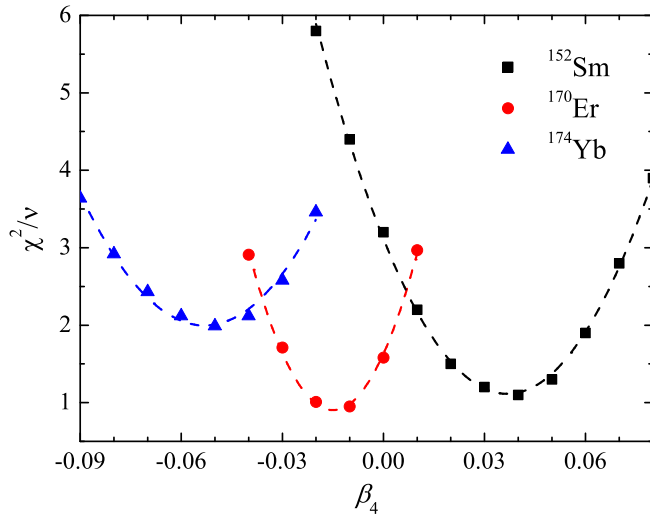


FIG. 4. (Color online) The χ^2/ν for the studied ^{152}Sm , ^{170}Er , and ^{174}Yb nuclei as a function of β_4 . The curves are the parabolic fittings for illustrating the determination of the optimal values and (fitting) uncertainties of the β_4 parameters.

optimal β_4 values, χ^2 analysis has been performed with only one free parameter. Figure 4 shows the χ^2/ν varying with the β_4 values in fitting the lower energy QEL scattering excitation functions, where $\nu = pt - 1$ is the degree of freedom of the χ^2 distribution, pt denotes the number of measurement points. For a good measurement and a suitable physical model, the variation of χ^2/ν with the fitted parameter follows a parabola [43], as shown in Fig. 4. The optimal β_4 values are determined by χ_{\min}^2 . Since the χ^2/ν is much larger than 1 for the ^{174}Yb case (see Table II), the uncertainty was calculated using $\chi_{\min}^2 + \chi_{\min}^2/\nu$ [44]. For the ^{152}Sm and ^{170}Er , where the χ^2/ν is close to 1, the uncertainties were calculated using $\chi_{\min}^2 + 1$.

Figure 5 represents part of the available results of β_4 for the Sm, Er, and Yb isotopes as a function of N by using different methods. Charge deformation parameters β_4^C (α^C) extracted by means of Coulomb excitation [18,39,40,42]. Nuclear deformation parameters β_4^N (α^N) by using the interference effects between Coulomb and nuclear excitations [38], and the inelastic scattering of α at energies well above the barrier [18,21]. Also included in this plot are the β_4 parameters of $^{152,154}\text{Sm}$, ^{166}Er , and ^{176}Yb obtained from electron scattering (e^-) [22].

TABLE II. The extracted β_4 from the lower-energy backward QEL excitation function.

Nucleus	β_4	χ_{\min}^2/ν
^{152}Sm	0.037(0.006)	1.1
^{170}Er	-0.015(0.004)	0.9
^{174}Yb	-0.053(0.009)	2.0

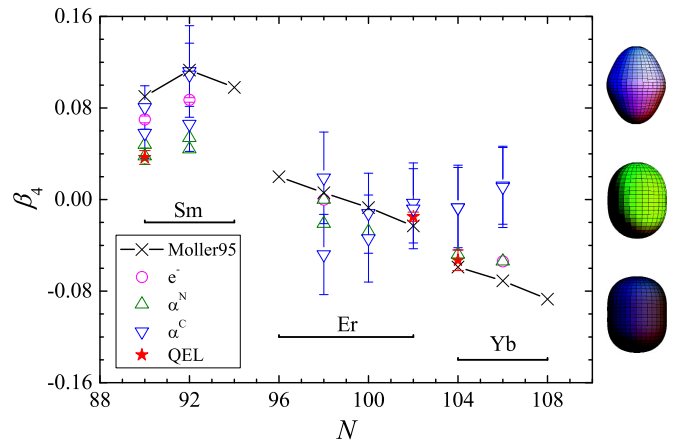


FIG. 5. (Color online) The variation of β_4 with N for the Sm, Er, and Yb isotopes by using different experimental methods and Möller's theoretical prediction [26]. Three schematic forms corresponding to $\beta_4 = -0.1, 0$, and 0.1 with $\beta_2 = 0.3$ are illustrated, respectively.

Deformation parameters of the nuclear ground states calculated in the spherical-harmonics expansion with a macroscopic-microscopic model [26] are also shown in Fig. 5. Compared with β_4^C , β_4^N has a good consistency and roughly follows the theoretical prediction. The extracted β_4 parameters in this work are also plotted (solid points) and qualitatively agree with the overall trend. This result suggests the feasibility of extracting β_4 from sub-barrier backward QEL scattering.

It should be pointed out that these extracted β_4 parameters are all model dependent and hence have uncertainties [21,22,39]. For the present work, the selection of coupling scheme like the number of excitation states and transfer channels may bring about an uncertainty for the extracted deformation parameters. The accumulation of abundant model-dependent values, however, may help to judge a true and model-independent value.

In summary, we have measured the QEL scattering excitation functions with high statistics at a backward angle and extracted the barrier distributions for $^{16}\text{O} + ^{152}\text{Sm}$, ^{170}Er , and ^{174}Yb . An attempt was made to extract β_4 by using the lower energy experimental QEL excitation function for the first time, based on the fixed β_2 with the help of the CC calculations. The extracted β_4 shows a transition from positive for ^{152}Sm , to near zero for ^{170}Er , to negative for ^{174}Yb , which is consistent with the available trend qualitatively. This may offer a simple but sensitive method to extract β_4 . Further, this work suggests a promising way to extract β_4 , with the increasing experimental knowledge of quadrupole collectivity [28–30], of the radioactive nuclei from the sub-barrier backward QEL scattering.

ACKNOWLEDGMENTS

This work has been supported by the National Key Basic Research Development Program of China under Grant No. 2013CB834404 and the National Natural Science Foundation of China under Grants No. 11375268 and No. 10735100.

- [1] R. G. Stokstad *et al.*, *Phys. Rev. Lett.* **41**, 465 (1978).
- [2] L. F. Canto, P. R. S. Gomes, R. Donangelo, and M. S. Hussein, *Phys. Rep.* **424**, 1 (2006).
- [3] M. Dasgupta, D. J. Hinde, N. Rowley, and A. M. Stefanini, *Annu. Rev. Nucl. Part. Sci.* **48**, 401 (1998).
- [4] N. Rowley, G. R. Satchler, and P. H. Stelson, *Phys. Lett. B* **254**, 25 (1991).
- [5] J. X. Wei *et al.*, *Phys. Rev. Lett.* **67**, 3368 (1991).
- [6] A. M. Stefanini *et al.*, *Phys. Rev. Lett.* **74**, 864 (1995).
- [7] C. R. Morton *et al.*, *Phys. Rev. Lett.* **72**, 4074 (1994).
- [8] H. Timmers *et al.*, *Nucl. Phys. A* **584**, 190 (1995).
- [9] L. R. Gasques *et al.*, *Phys. Rev. C* **76**, 024612 (2007).
- [10] M. J. Rhoades-Brown and V. E. Oberacker, *Phys. Rev. Lett.* **50**, 1435 (1983).
- [11] H. Esbensen and S. Landowne, *Nucl. Phys. A* **467**, 136 (1987).
- [12] J. R. Leigh, J. J. M. Bokhorst, D. J. Hinde, and J. O. Newton, *J. Phys. G* **14**, L55 (1988).
- [13] J. Fernández-Niello and C. H. Dasso, *Phys. Rev. C* **39**, 2069 (1989).
- [14] M. A. Nagarajan, A. B. Balantekin, and N. Takigawa, *Phys. Rev. C* **34**, 894 (1986).
- [15] R. C. Lemmon *et al.*, *Phys. Lett. B* **316**, 32 (1993).
- [16] J. R. Leigh *et al.*, *Phys. Rev. C* **47**, R437 (1993).
- [17] J. R. Leigh *et al.*, *Phys. Rev. C* **52**, 3151 (1995).
- [18] I. Y. Lee *et al.*, *Phys. Rev. C* **12**, 1483 (1975).
- [19] F. Todd Baker *et al.*, *Nucl. Phys. A* **258**, 43 (1976).
- [20] F. Todd Baker *et al.*, *Nucl. Phys. A* **266**, 337 (1976).
- [21] D. L. Hendrie *et al.*, *Phys. Lett. B* **26**, 127 (1968).
- [22] T. Cooper *et al.*, *Phys. Rev. C* **13**, 1083 (1976).
- [23] R. J. Powers *et al.*, *Phys. Rev. Lett.* **34**, 492 (1975).
- [24] P. Möller, *Nucl. Phys. A* **142**, 1 (1970).
- [25] U. Götze, H. C. Pauli, K. Alder, and K. Junker, *Nucl. Phys. A* **192**, 1 (1972).
- [26] P. Möller, J. R. Nix, W. D. Myers, and W. J. Swiatecki, *At. Data Nucl. Data Tables* **59**, 185 (1995).
- [27] J. O. Fernández Niello *et al.*, *Phys. Rev. C* **43**, 2303 (1991).
- [28] S. Ilieva *et al.*, *Phys. Rev. C* **89**, 014313 (2014).
- [29] M. Seidlitz *et al.*, *Phys. Rev. C* **89**, 024309 (2014).
- [30] S. Michimasa *et al.*, *Phys. Rev. C* **89**, 054307 (2014).
- [31] C. J. Lin *et al.*, *Phys. Rev. C* **79**, 064603 (2009).
- [32] K. Hagino, N. Rowley, and A. T. Kruppa, *Comput. Phys. Commun.* **123**, 143 (1999).
- [33] C. J. Lin *et al.*, *EPJ Web Conf.* **17**, 05005 (2011).
- [34] K. Hagino and N. Rowley, *Phys. Rev. C* **69**, 054610 (2004).
- [35] K. Hagino, T. Takehi, A. B. Balantekin, and N. Takigawa, *Phys. Rev. C* **71**, 044612 (2005).
- [36] S. Raman, C. W. Nestor, Jr., and P. Tikkanen, *At. Data Nucl. Data Tables* **78**, 1 (2001).
- [37] K. Hagino, N. Takigawa, M. Dasgupta, D. J. Hinde, and J. R. Leigh, *Phys. Rev. Lett.* **79**, 2014 (1997).
- [38] W. Brückner, J. G. Merdinger, D. Pelte, U. Smilansky, and K. Traxel, *Phys. Rev. Lett.* **30**, 57 (1973).
- [39] H. Fischer *et al.*, *Phys. Rev. C* **15**, 921 (1977).
- [40] K. A. Erb, J. E. Holden, I. Y. Lee, J. X. Saladin, and T. K. Saylor, *Phys. Rev. Lett.* **29**, 1010 (1972).
- [41] D. L. Hendrie, *Phys. Rev. Lett.* **31**, 478 (1973).
- [42] H. J. Wollersheim, W. Wilcke, and T. W. Elze, *Phys. Rev. C* **11**, 2008 (1975).
- [43] L. Lyons, *Statistics for Nuclear and Particle Physicists* (Cambridge University Press, Cambridge, 1986).
- [44] P. McCullagh and J. A. Nelder, *Generalized Linear Models*, 2nd ed., Monographs on Statistics and Applied Probability (CRC, Boca Raton, FL, 1989).